1EV GaN[subscript x]As[subscript 1-x-y]Sb[subscript y] material for lattice-matched III-V solar cell implementation on GaAs and Ge

1EV $GAN_xAS_{1-x-y}SB_y$ MATERIAL FOR LATTICE-MATCHED III-V SOLAR CELL IMPLEMENTATION ON GAAS AND GE

Tien Khee Ng[1], Soon Fatt Yoon[1,2], Kian Hua Tan[1], Wan Khai Loke[1], Satrio Wicaksono[1], Kim Luong Lew[1], Kah Pin Chen[1,2], Eugene A. Fitzgerald[3,4], Arthur J. Pitera[3], Steve A. Ringel[5], Andrew M. Carlin[5], and Maria Gonzalez[5]

[1] School of Electrical and Electronic Engineering, Nanyang Technological University, Nanyang Avenue, Singapore 639798, Singapore.

[2] Singapore-MIT Alliance, N3.2-01-36, 65 Nanyang Drive, Singapore 637460, Singapore.

[3] Department of Materials Science and Engineering, Massachusetts Institute of Technology, 77 Massachusetts Avenue, Cambridge, Massachusetts 02139, USA.

[4] Singapore-MIT Alliance, Room 8-407, 77 Massachusetts Avenue, Cambridge, Massachusetts 02139, USA.

[5] Department of Electrical and Computer Engineering, The Ohio State University, Columbus, Ohio 43210, USA.

ABSTRACT

The effect of different arsenic species (As_2 or As_4) on the quality of molecular beam epitaxy (MBE) grown GaNAsSb materials (samples A and B) and GaAs/ GaNAsSb/GaAs $p^+ n^- n^+$ devices (samples C and D) were investigated. The improvement in material quality in sample B, as well as the improvement in diode and solar cell characteristics in sample C, may suggest a successful defect density manipulation using As_2 overpressure for GaNAsSb growth.

INTRODUCTION

In the III-V photovoltaic sector, the implementation of III-V compound semiconductor lattice-matched to GaAs or Ge, and with bandgap in the 0.9 - 1 eV range is especially attractive due to its potential in realizing high energy conversion efficiency leading towards >40-50 %.[1] The research methodology towards this goal is to improve the 1 sun energy conversion efficiency of a multijunction solar cell application, and then employ solar concentrator technique to boost energy conversion efficiency and to reduce cell cost. One important effort involved the implementation of lattice-matched 0.9-1 eV in the existing 40.7% efficient AlGaInP/GaInAs/Ge triple-junction solar cell to improve the spectral utilization of sunlight. In this respect, the dilute nitride material is one potential candidate [2]. However, this effort had suffered from the difficulty in growing high quality 0.9 – 1 eV $Ga_{1-y}In_yN_xAs_{1-x}$ layer with y = 3x. For example, a high unintentional carrier concentration in the GaInNAs layer led to a low carrier mobility and diffusion length [3]. Other GaInNAs related devices implementations were usually hampered by short minority carrier lifetime in bulk GaInNAs material due to the presence of deep level traps [4]. A short minority carrier lifetime (τ) is associated with a larger recombination related reverse saturation current (J_o) with ideality factor (n) much larger than 1, which will in turn lead to smaller open circuit voltage (V_{oc}).[5] To date, there is a lack of success in the use of lattice-matched dilute nitride in multijunction III-V solar cell applications [2,4]. Hence, more scientific investigation will be required to solve the current issue.

This research focuses on the implementation of GaNAsSb for solar cell applications to fill the research gap in GaAs- and Ge-lattice-matching 1 eV solar cell applications. In order to avoid the detrimental effect of In-N clustering and embrace the beneficial effect of Sb [6] in possibly reducing the N migration and hence suppressing the formation of N-complex [7,8], indium were avoided. Also, unlike GaInNAs laser applications, where a high compressive-strain was required and was achieved by In composition of ~40%,[7] dilute-nitride solar cell layer structure lattice-matched to GaAs or Ge does not need the incorporation of indium, and lattice-matched GaNAsSb can be achieved by simply tuning the N, As and Sb composition, as demonstrated in this paper.

EXPERIMENTAL METHODS

In this study, a molecular beam epitaxy (MBE) system in conjunction with radio-frequency (RF) nitrogen plasma was used to grow GaNAsSb materials. The GaNAsSb growth process was modified [9] from earlier experiences in 0.94 eV GanAsSb photodetector work [10,11]. By tuning the compositions of N, As and Sb in the GaNAsSb material, one can achieve ~1 eV semiconductor energy gap and lattice-matching to GaAs or Ge substrate simultaneously. The samples A - D discussed in this paper were grown on (001) GaAs substrate. Nevertheless, the growth process for transferring the III-V layers onto Ge-terminating substrate has already been developed earlier [12] for future integration onto Ge substrate or SiGe-based substrate.

The first part of this investigation will present the characterization of GaNAsSb / GaAsSb material structure in sample A and sample B by X-ray diffraction (XRD) in order to confirm that the desired material characteristics

978-1-4244-2950-9/09/$25.00 ©2009 IEEE

were achieved. The photoluminescence (PL) spectroscopy was then used to examine the quality of GaNAsSb materials grown under As_4 and As_2 overpressure in sample A and B, respectively.

The current transport mechanisms of GaAs / ~1eV-GaNAsSb / GaAs $p^+ n^- n^+$ devices, namely sample C and sample D, were investigated with the GaNAsSb grown under As_2 overpressure and As_4 overpressure, respectively. The n^- ~1eV-GaNAsSb layer were grown at ~400 ℃, and whereas the growth temperature for the GaAs layers were 580 ℃. It is noted that the 580 ℃ temperature may have introduced some annealing effect into the devices.

RESULTS AND DISCUSSIONS

The GaNAsSb layer will be closely matched to GaAs as long as the N composition is ~2.8 times the Sb composition. By growing the undoped GaNAsSb / GaAsSb double-layer structure on (001) GaAs substrate, the N and Sb compositions can be conveniently determined during X-ray diffraction (XRD) dynamical theory simulation using the strain-balance effect of N and Sb incorporation (see Figure 1(a)). The GaAsSb layer was grown to estimate the Sb composition and the N composition was then estimated by taking the same Sb composition for the GaNAsSb layer during the above simulation. Sample A has N = 1.25% and Sb = 5.7% while sample B has N = 1.6% and Sb = 6% as determined from XRD dynamical theory simulation (see dotted curves in Figure 1). The results showed that low and comparable lattice-mismatch values of 0.19% and 0.14% were successfully achieved for samples A and B, respectively. Since the N composition in sample B's GaNAsSb layer (1.6%) is higher than that of sample A (1.25%), it is expected that the full-width at half-maximum (FWHM) of the photoluminescence (PL) spectra for the GaNAsSb layer in sample B will therefore be larger compared to that of sample A.[8]

On the contrary, Figure 2 showed the 5K PL full-width at half-maximum (FWHM) values for GaNAsSb in sample A (65 meV) was larger than that of sample B (60 meV). Since As_4 and As_2 overpressure were used during the growth of GaNAsSb in sample A and sample B, respectively, it was believed that the As_2 species suppressed the existence of certain point defects that gave rise to non-radiative recombination center (or defect center), leading to a narrower FWHM in the GaNAsSb layer in sample B.

To obtain further scientific insight into the role of the above defect center in GaNAsSb device, the electrical characteristics of GaAs / ~1eV-GaNAsSb / GaAs $p^+ n^- n^+$ devices, namely sample C and sample D, were investigated. The 0.25 mm^2 vertical diode structures with top and bottom *Ohmic* contacts were used for this purpose.

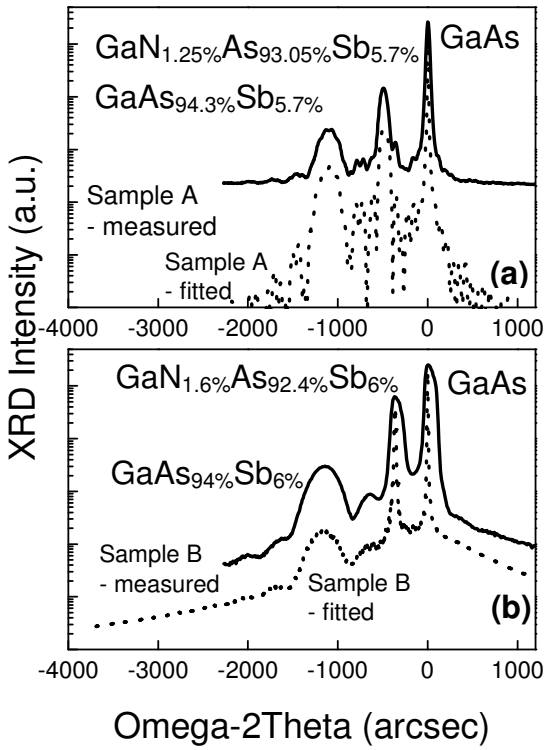

Figure 1: Plot of (004) X-ray diffraction curves for: (a) sample A, and (b) sample B, which were grown under As_4 and As_2, respectively.

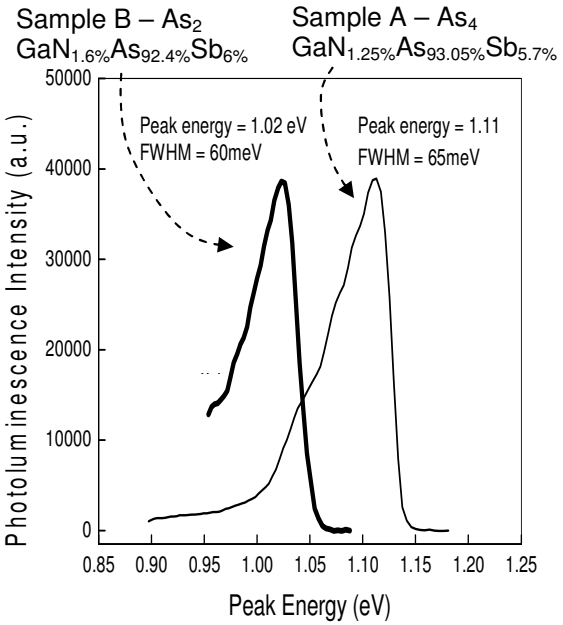

Figure 2: Plot of 5K photoluminescence spectrum of the GaNAsSb layers in sample A and sample B, which were grown under As_4 and As_2 overpressure, respectively.

As mentioned, the 1eV GaNAsSb layer in sample C and sample D were grown under As_2 overpressure and As_4 overpressure, respectively, and by keeping all other growth conditions constant. It is known that As_2 have larger sticking coefficient value compare to As_4 during GaAs growth, and the use of As_2 was found to promote 2D nucleation growth mode during GaNAs grow [13], which resulted in an improve PL characteristics. It is believe that this will similarly affect the growth kinetics of the GaNAsSb layer in sample C and sample D, and resulted in a lower defect density in sample C.

As a result, it is expected that the carrier dynamics in both samples will also be different. This is evident in Figure 3(a) and (b), where the reverse dark current density at -2V ($J_{r,dark,-2V}$) for sample C (~10^{-6} A/cm^2) was significantly lower than that of sample D (~10^{-2} A/cm^2). This indicated a significant contribution of a dominant recombination-generation center (RG center), in sample D with the GaNAsSb layer grown under As_4 overpressure. This is further supported by the observation at 0.3 V forward bias voltage ($J_{f,dark,0.3V}$), where sample C showed a larger ideality factor, n ~ 1.46, while sample D showed n ~ 1.6, indicating a larger effect of RG center in sample D. The observations were consistent with the results obtained from the PL FWHM study in Figure 2.

The RG center was detrimental to the minority carrier lifetime (τ), and the higher RG current may reduce the open-circuit voltage (V_{oc}) in solar cell implementation. To estimate the degree of change in the minority carrier lifetime, It is noted that the typical diode *current density (J) – voltage (V)* equation consisted of the following double exponential terms, with the first and second exponential terms representing the diffusion and recombination-generation current density components [14], respectively:

$$J = J_{01}.e^{qVa/kT} + J_{02}.e^{qVa/2kT} \qquad (1)$$

J_{01} and J_{02} are the saturation current density component for n close to 1 and 2, respectively, while, q, V_a, k and T have their usual meaning, *i.e.* applied voltage, Boltzmann constant and absolute temperature, respectively.

With n values much greater than 1 in Figure 3, the *J-V* characteristics of sample C and D were both much affected by the recombination-generation current components; though a smaller n of 1.46 indicated that sample C was less affected by RG center compared to sample D. To quantify this effect, it is noted that the RG center related saturation current density at a reverse bias voltage of a few kT/q can be approximated by the following equation, with n_i, W_d, and τ represent the intrinsic carrier concentration, depletion width and carrier lifetime under the influence of RG center, respectively: [14]

$$J_{02} = (q\, n_i\, W_d) / (2\, \tau) \qquad (2)$$

The saturation current density for sample C and D are J_{02_C} ~ 1x10^{-6} A/cm^2 and J_{02_D} ~ 1x10^{-4} A/cm^2, respectively, near the origin. If it is assumed here that the n_i values are similar for both GaNAsSb material, and the introduction of defects will only affect W_d and τ. To evaluate W_d, the capacitance *vs.* voltage characteristics for the diode structure for sample C and D were measured. The capacitance and the corresponding depletion width for sample C near 0 V were 47 pF and ~500nm (*i.e.* fully depleted), respectively; while that of sample D were 92 pF and ~300 nm, respectively. This will then translate into recombination lifetime of sample C much longer than that of sample D by ~170x. A shorter lifetime for sample D may point to a higher density of RG center.

The above discussions are by no means complete and this is our first attempt to demonstrate an improvement in the GaNAsSb material for solar cell implementation. Therefore there are still many questions that need to be answered to fully understand the observation reported here. The time-resolved PL measurements will be required to verify the change in lifetime as a result of the change in defect density under the influence of As_2 or As_4 species. It is also noted that the exact origin of the RG center or defect center will require further deep level transient spectroscopy (DLTS) investigation, and will be reported in due course.

Nevertheless, the beneficial effect of growing GaNAsSb under As_2 species has been clearly demonstrated in this paper. This represents a significant milestone in GaNAsSb

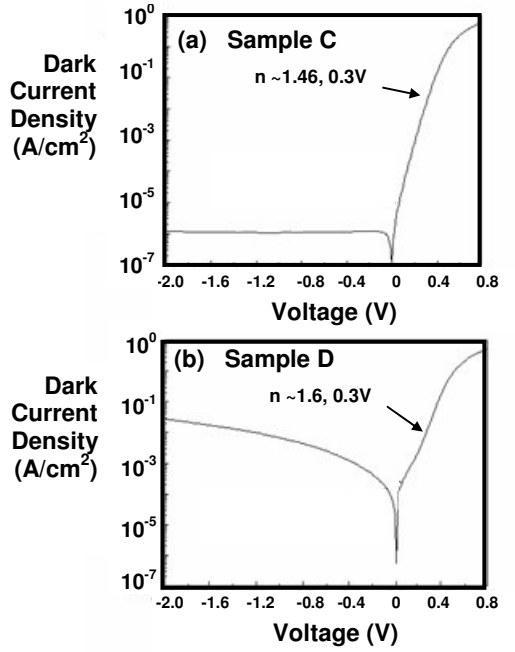

Figure 3: Dark current density *vs.* voltage characteristics of: (a) sample C with GaNAsSb layer grown under As_2 overpressure, and (b) sample D with GaNAsSb layer grown under As_4 overpressure.

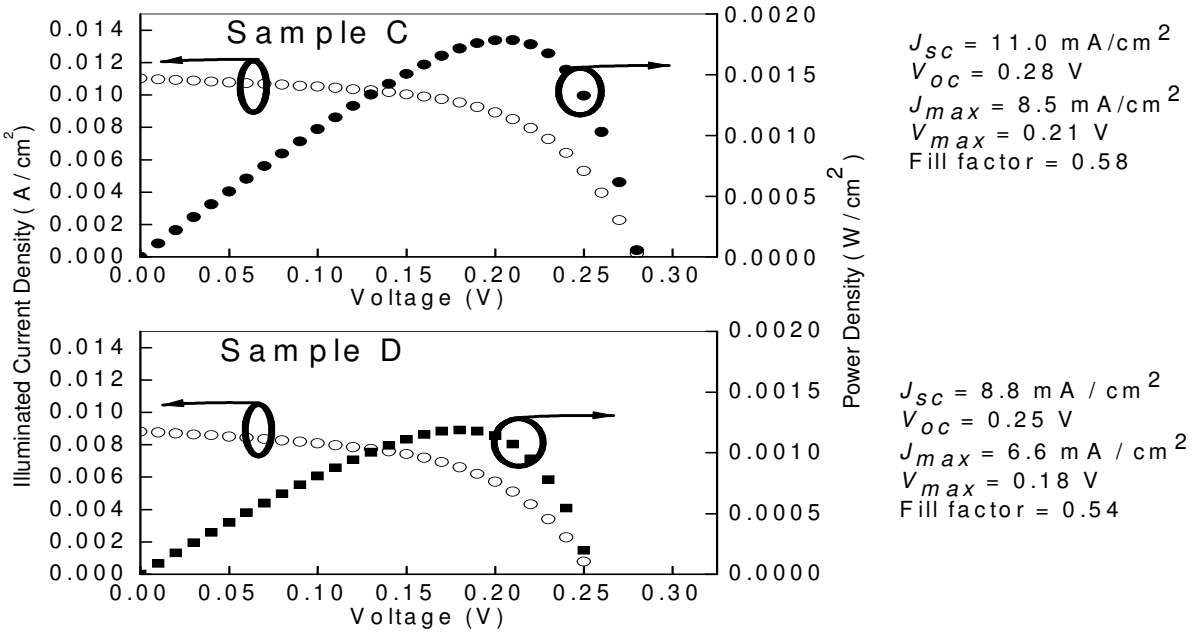

Figure 4: One sun illuminated current density and power density *vs.* voltage characteristics of: (a) sample C with GaNAsSb layer grown under As_2 overpressure, and (b) sample D with GaNAsSb layer grown under As_4 overpressure.

material research and the newly discovered process conditions can potentially be a viable method to solve a similar problem faced in dilute-nitride research. Such improvement is likely due to a reduction in a major defect density within the 1 eV GaNAsSb material. Again, this will required further deep level transient spectroscopy (DLTS) investigation to ascertain the characteristics of the contributing defect center.

Finally, the GaNAsSb solar cell characteristic in sample C showed a consistent improvement when the one sun illuminated *J-V* curve of the 4.4 mm^2 solar cells were examined. The 4.4 mm^2 solar cell pattern discussed in Figure 4 and the 0.25 mm^2 diode pattern discussed in Figure 3 were designed on the same masks so that both can be fabricated on the same wafer in one process run. The figure of merits (FOM) for samples C and D are shown in Figure 4(a) and 4(b), respectively. The figures-of-merit (FOM), such as J_{sc}, V_{oc}, J_{max}, V_{max} and fill factor, for sample C were much more superior than that of sample D, respectively, due to the use of As_2 species during the growth of GaNAsSb layer.

CONCLUSIONS

This work represents the first intentional attempt to discard indium in the implementation of 1eV dilute nitride solar cell lattice-matched to GaAs or Ge. The GaNAsSb PL FWHM characteristic, as well as diode and solar cell *J-V* results suggested that RG center or defect center can be significantly suppressed by changing the As species to As_2. A consistent improvement was also demonstrated in the much improved solar cell FOMs for sample C. Moving forward, the characteristics of the above-mentioned RG center will be identified so that further defect control methodologies can be discovered.

ACKNOWLEDGEMENT

The authors gratefully acknowledge the support from National Research Foundation and Economic Development Board, Singapore, for this research under the project ID NRF2007EWT-CERP01-0206.

REFERENCES

[1] D.J. Friedman, S R. Kurtz, and J.F. Geisz, “Analysis of the GaInP/GaAs/1-eV/Ge cell and related structures for terrestrial concentrator application”, *Conference Record of the Twenty-Ninth IEEE Photovoltaic Specialists Conference*, pages 856-859 (19-24 May 2002).

[2] J.F. Geisz, D.J. Friedman, J.M. Olson, S.R. Kurtz, and B.M. Keyes, “Photocurrent of 1 eV GaInNAs lattice-matched to GaAs”, *Journal of Crystal Growth*, **195**, page 401-408 (1996).

[3] F. Dimroth, C. Baur, A.W. Bett, K. Volz, and W. Stolz, “Comparison of dilute nitride growth on a single-and 8x4-inch multiwafer MOVPE system for solar cell applications”, *Journal of Crystal Growth*, **272**, page 726–731 (2004).

[4] W.K. Loke, S.F. Yoon, K.H. Tan, S. Wicaksono, and W.J. Fan, “Improvement of GaInNAs p-i-n photodetector responsivity by antimony incorporation”, *Journal of Applied Physics*, **101(3)**, page 033122 (2007).

[5] C.L. Andre, M. Wilt, A.J. Pitera, M.L. Lee, E.A. Fitzgerald, and S.A. Ringel, “Impact of dislocation densities on n+ / p and p+ / n junction GaAs diodes and solar cells on SiGe virtual substrate”, *Journal of Applied Physics*, **98**, page 014502 (2005).

[6] J.S. Harris Jr., R. Kudrawiec, H. B. Yuen, S. R. Bank, H. P. Bae, M. A. Wistey, D. Jackrel, E. R. Pickett, T. Sarmiento, L. L. Goddard, V. Lordi, and T. Gugov, “Development of GaInNAsSb alloys: Growth, band structure, optical properties and applications”, *Physica Status Solidi (b)*, **244(8)**, 2707–2729 (2007).

[7] H.B. Yuen, S.R. Bank, M.A. Wistey, J.S. Harris, and A. Moto, "Comparison of GaNAsSb and GaNAs as quantum-well barriers for GaInNAsSb optoelectronic devices operating at 1.3-1.55 μm", *Journal of Applied Physics*, **96**, page 6375 (2004).

[8] T.K. Ng, S.F. Yoon, S.Z. Wang, L.-H. Lin, Y. Ochiai, and T. Matsusue, “Photoluminescence Characterization of GaInNAs/GaAs Quantum Well Carrier Dynamics”, *Journal of Applied Physics*, **94(5)** 3110-3114 (2003).

[9] K.H Tan (Nanyang Technological University, Singapore), private communication.

[10] K.H. Tan, S.F. Yoon, W.K. Loke, S. Wicaksono, K.L. Lew, A. Stöhr, O. Ecin, A. Poloczek, A. Malcoci, and D. Jäger, “High-speed picosecond pulse response GaNAsSb p-i-n photodetectors grown by RF plasma-assisted nitrogen molecular beam epitaxy”, *Applied Physics Letters*, **90(1)**, pages 183515:1-3 (2007).

[11] S. Wicaksono, S.F. Yoon, W.K. Loke, K.H. Tan, and B.K. Ng, "Effect of growth temperature on closely lattice-matched GaAsSbN intrinsic layer for GaAs-based 1.3 μm *p-i-n* photodetector", *Journal of Applied Physics*, **99**, pages 104502, (2006).

[12] T.K Ng, S.F. Yoon, K.H. Tan, K.P. Chen, H. Tanoto, K.L. Lew, S. Wicaksono, and W.K. Loke, C. Dohrman, and E.A. Fitzgerald, “Molecular Beam Epitaxy Growth of Bulk GaNAsSb on Ge/graded-SiGe/Si Substrate”, *Journal of Crystal Growth*, **311**, pages 1754-1757 (2009).

[13] A. Takata, R. Oshima, H. Shigekawa, and Y. Okada, “Growth of GaNAs films with As2 source in atomic hydrogen-assisted molecular beam epitaxy”, *Journal of Crystal growth*, **310**, pages 3710– 3713 (2008).

[14] *See for example*: Robert F. Pierret, *Semiconductor Device Fundamentals*, pages 272-273, Addison-Wesley Publishing Company Inc, USA (1996).